Delay-Time-Enhanced Flat-Band Photonic Crystal Waveguides with Capsule-Shaped Holes on Silicon Nanomembrane

Yun-Sheng Chen, *Student Member, IEEE*, Yang Zhao, *Student Member, IEEE*, Amir Hosseini, *Student Member, IEEE*, David Kwong, Wei Jiang, Seth R. Bank, *Member, IEEE*, Emanuel Tutuc, and Ray T. Chen, *Fellow, IEEE*

***Abstract*—A slow-group-velocity- and low-group-velocity-dispersion photonic crystal slab waveguide is designed by using capsule-shaped air holes in hexagonal lattice. The theoretical study shows that adjusting the aspect ratio of holes in the innermost rows can fine-tune the dispersion tail. The presented design can achieve nearly flat-band photonic crystal waveguides with group index of 21–36 over the normalized bandwidth ($\Delta\omega/\omega$) of 1.38%–0.4%. We also discuss the effects of the change in the holes' aspect ratio combined with a slight size adjustment. The group index in the range of 21–43 for normalized bandwidth of about 1.5%–0.3% is obtained with the combination effect. The optimized designed exhibits a nearly constant group index of 21 over 22.7 nanometer bandwidth at $\lambda = 1.55$ μm.**

***Index Terms*—Group velocity dispersion, photonic crystal waveguide, slow group velocity.**

I. Introduction

THE INTEREST in manipulating the speed of propagating light has increased dramatically in recent years for applications such as optical delay lines [1], optical buffers [2], [3], and all optical switches [4]. The possibility to compress the energy and signal provides the opportunity for reducing the footprint of the devices. In addition, the strong light–matter interaction due to the small group velocity enhances the absorptions, non linearity, and gains per unit length that benefits numerous optical devices, such as detectors, amplifiers, and lasers [5], [6]. In recent years, the engineered slow-light photonic crystals have drawn a great deal of attention by researchers because of the flexibility in design and compatibility for on-chip applications. Slow-light 3-D semiconductor photonic crystals with a complete band gap are ideal candidates, however their fabrication is challenging. Planar photonic crystal slabs fabricated on semiconductor membrane, such as silicon-on-insulator (SOI) wafers, where light is confined in-plane by the band gap of 2-D photonic crystals [7]–[9] or by 2-D negative refractive index photonic crystals [10] and vertically by total internal reflection of index contrast are alternative solutions because of their relative ease of fabrication. However, the narrow bandwidth due to the highly dispersive group velocity of the photonic crystal slabs in the slow-light regime restricts their applications [11]. Several research groups have achieved low group velocity dispersion (GVD) by adjusting the waveguide width [12]–[14], the size of the first two innermost rows of holes [15], [16], the displacement of the first two rows [17], or by chirping the property of photonic crystals [18]. In this paper, a design of photonic crystal slab waveguide with a nearly constant group index of 21 over 22.7 nm centered at $\lambda = 1.55$ μm is reported, which could provide an alternative path to approach the flat-band photonic crystal waveguides.

Manuscript received January 3, 2009; revised January 28 2009, March 5, 2009, and March 29, 2009. Current version published October 7, 2009. This work was supported by the multidisciplinary university research initiative (MURI) program through the Air Force Office of Scientific Research (AFOSR).

Y.-S. Chen, Y. Zhao, A. Hosseini, D. Kwong, S. R. Bank, E. Tutuc, and R. T. Chen are with the Microelectronic Research Center, Department of Electrical and Computer Engineering, University of Texas at Austin, Austin, TX 78758 USA (e-mail: yunshengchen@gmail.com; zhaoyang1008@gmail.com; amir_h1982@yahoo.com; diddykwong@gmail.com; sbank@ece.utexas.edu; etutuc@mail.utexas.edu; chen@ece.utexas.edu).

W. Jiang is with the Department of Electrical and Computer Engineering and the Institute for Advanced Materials, Devices and Nanotechnology, Rutgers University, Piscataway, NJ 08854 USA (e-mail: wjiangnj@rci.rutgers.edu).

Color versions of one or more of the figures in this paper are available online at http://ieeexplore.ieee.org.

Digital Object Identifier 10.1109/JSTQE.2009.2020811

II. Design of Photonic Crystal Slab Waveguide

An air-bridged silicon photonic crystal slab waveguide with a hexagonal lattice and "capsule" shaped air holes is considered in the calculations. As shown in Fig. 1(a), a, t, $2r + l$, and $2r$ denote the periodicity, the slab thickness, the total length of capsule, and the width of the capsule, respectively. The refractive index of the slab n is 3.46 at $\lambda = 1.55$ μm and t is $0.6a$. The slab is laid on the x–z plane and a line waveguide is formed by removing a single row of holes along x-direction in real space that is corresponding to the ΓK-direction of the reciprocal lattice. Due to the introduction of the line defect, the Brillouin Zone edge is shifted from K to K′ instead [19]. The band structure of the photonic crystal, as illustrated in Fig. 1(b), is calculated using BandSOLVE^{TM} of the Rsoft Photonics CAD Design Suite based on 3-D plane-wave-expansion (PWE) method and projected from the ΓM-direction onto the ΓK′-direction, which gives the boundary of the first Brillouin zone. The defect modes inside the band gap are studied by replacing a 1×1 unit cell with a supercell that is 1 unit in the x-direction and 6 units in the z-direction in the PWE calculation, as shown in the inset of Fig. 1(b). The figure also shows a lateral even-guided mode and a lateral odd-guided mode, and both of them are vertical even modes. The vertical even mode is defined as the mode symmetric with respect to the x–z plane. The lateral even-guided mode is defined as the mode symmetric with respect to the x–y plane, which is a fundamental mode, while the lateral odd-guided mode

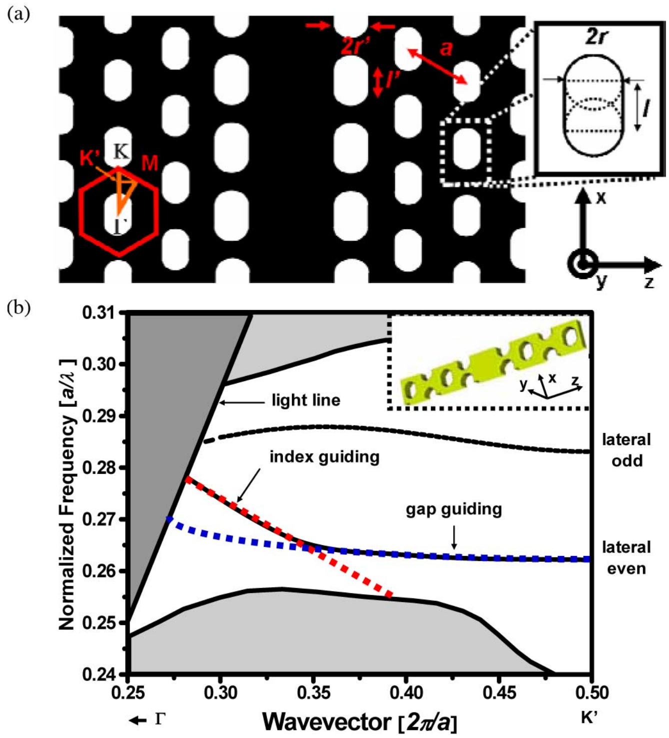

Fig. 1. (a) Geometry of the capsule-shaped hole photonic crystal waveguide with hexagonal lattice. Two half circles with diameter of *2r* at both terminals and a rectangle with a width of *2r* and length of *l* in the middle assemble the capsule. (b) Typical band diagram of the capsule-shaped photonic crystal. The red dot line indicates the index-guided regime and blue dot curve shows the gap-guided regime. The inset illustrates the 1×6 supercell in plane, which has six periods in the vertical direction to ensure that the defect is sufficiently isolated.

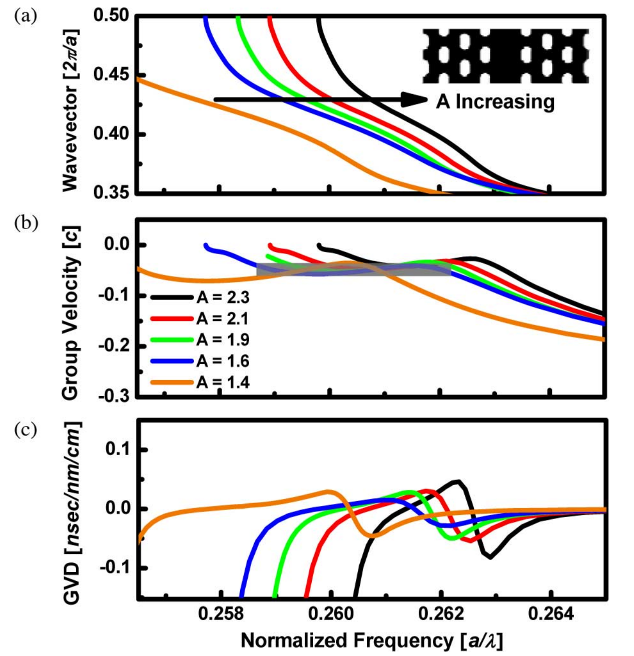

Fig. 2. (a) Waveguide mode dispersion with various aspect ratios that are larger than one, with fixed area ratio R equal to one. The guiding modes move toward higher frequency as the aspect ratio is increased. (b) Corresponding group velocities of the guided modes. The gray bar marked the regime that the group velocity fluctuation is within $\pm 10\%$. (c) Corresponding GVD of the guided modes indicate that in the flat-band regime the GVD fluctuation is smaller than ± 0.07 ns/(nm·cm) for the case of $A = 2.3$, and is smaller than ± 0.05 ns/(nm·cm) for the rest cases.

is a higher order mode. The group velocity of a guided mode is calculated from its definition as the derivative of the angular frequency over the wavevector

$$\upsilon_g \equiv \frac{\partial \omega}{\partial k}. \tag{1}$$

The derivative of the reciprocal group velocity over the frequency gives the GVD

$$\text{GVD} = \frac{\partial(1/\upsilon_g)}{\partial \lambda}. \tag{2}$$

In photonic crystal slab waveguide modes, there coexist gap-guided modes and index-guided modes. A high GVD happens at the anticrossing point, where gap-guided modes and index-guided modes couple with each other [11]. One can tailor the dispersion curve and shift the anticrossing point by engineering the parameters of the line defect. Frandsen *et al.* have proposed an approach to "flatten" the dispersion curve by perturbing the size of the periodic holes of the two innermost rows close to the defect [15]. An alternative new approach that this paper presents, aims to control the shift of gap-guided mode, thus flattening the dispersion curve by manipulating the aspect ratio of the capsule-shaped air holes.

The aspect ratio of the capsule-shaped holes is defined as

$$A = \begin{cases} \dfrac{2r' + l'}{2r'}, & A > 1 \\[2mm] \dfrac{2r'}{2r' + l'}, & A < 1 \end{cases} \tag{3}$$

where r is the radius of curvature at the two terminals of the capsule, and l is the length of the straight portion of the capsule as shown in Fig. 1(a). r' especially denotes that of the innermost rows, and so does l'. The dispersion relations of the calculated fundamental modes with various values of A are illustrated, respectively, in Fig. 2(a) and Fig. 3(a) under two different conditions. Corresponding schematic structures of the photonic crystal waveguide with aspect ratio of the holes bigger than 1 and smaller than 1 are shown in the insets of Fig. 2(a) and Fig. 3(a) accordingly. Aspect ratios of outside holes except for the innermost rows are fixed during the calculation, where the radius r is $0.162a$, the length l is $0.35a$, which corresponds to an aspect ratio of 2.08, and area of the hole of $0.196a^2$. The area ratio, which is defined as R, denotes the relative area ratio of innermost holes over outside holes

$$R = \frac{\pi r'^2 + 2r'l'}{\pi r^2 + 2rl}. \tag{4}$$

In the calculations of Figs. 2 and 3, R is kept as 1, which indicates that all the capsule holes have the same size irrespective of their locations in the waveguide. Under this condition, the designed photonic crystal waveguide can provide a

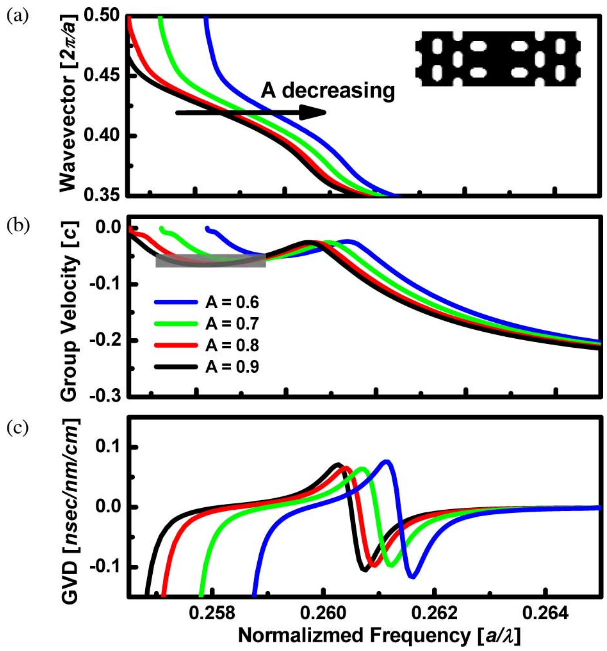

Fig. 3. (a) Waveguide mode dispersion with various aspect ratios that are smaller than one, with fixed area ratio R equal to one. The guided modes move toward higher frequency as the aspect ratio is decreased. (b) Corresponding group velocities of the guided modes. The gray bar marked the regime that the group velocity fluctuation is within ±10%. (c) Corresponding GVD of the guiding modes that indicate that in the flat-band regime the GVD fluctuation is smaller than ±0.1 ns/(nm·cm).

sufficient bandgap width for operation wavelength at 1.55 μm with corresponding periodicity within 400–450 nm.

III. Results and Discussions

To observe the effect of tuning the aspect ratio of holes at the innermost rows on the dispersion relation, group velocity as well as the GVD, aspect ratios of the innermost holes are changed with a fixed area equal to the outside holes. Aspect ratios of 1.4, 1.6, 1.9, 2.1, and 2.3 are chosen as an example. The trend is clear as A increases, both the index-guided mode and gap-guided mode move toward higher frequency, but with the tendency that the gap-guided modes moving faster than the index-guided mode, a sharper GVD happens at a lower wavevector when A increases. Fig. 2(b) and (c) shows two sets of comparison of group velocity and GVD, respectively, at the aforementioned aspect ratios. The GVD tends to vanish as A decreases, but increase after $A = 1.6$.

An aspect ratio smaller than 1 is realized by rotating the holes of the innermost rows close to the line defect 90° around the center of the hole, which is shown as the inset of Fig. 3(a), and A is defined as in (3). When $A < 1$, the trend of dispersion relation is opposite. It is when A decreases, that the gap-guided regime will move toward a higher frequency and form a sharp dispersion. Corresponding dispersion relation, group velocity and GVD with aspect ratios of 0.6, 0.7, 0.8, and 0.9 are shown in Fig. 3(b) and (c) to illustrate such phenomenon. These aspect ratios are reciprocals of 1.67, 1.43, 1.25, and 1.11. For instance, if A changes from 0.6 to 0.7, it can be considered to change an amount of 16.67%, which is similar to the degree of change when

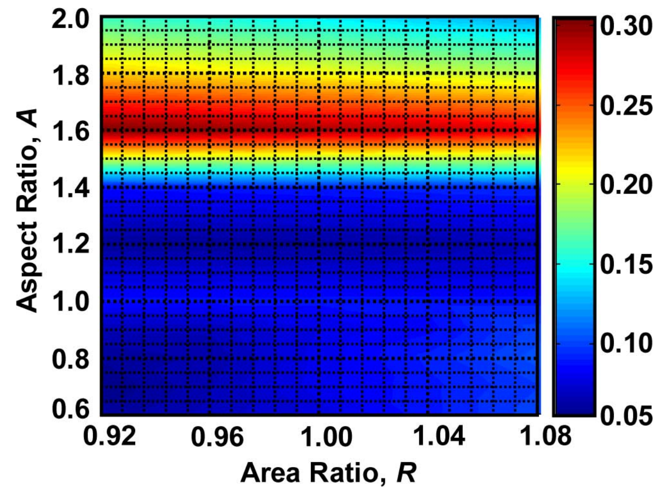

Fig. 4. Systematic calculation of product $n_g(\Delta\omega/\omega)$ as a function of area ratio R and aspect ratio A. The color bar indicates the product that is calculated to be within 0.03 to 0.3, when R is in the range of 0.92 to 1.08 and A is from 0.6 to 2.0.

A changes from 1.6 to 1.9 in $A > 1$ case. However, with the same amount of change in aspect ratio, when $A < 1$, Fig. 3(a) shows that gap-guided regime moves much faster than under the $A > 1$ case, which indicates that with a small aspect ratio (<1) of the innermost holes, the gap-guided modes are more sensitive to the change of the aspect ratio. Furthermore, one can observe that in the case of $A > 1$, the designed structure can control the GVD within 0.05 ns/(nm·cm) with properly chosen aspect ratio with group index around 30.

The effect of the manipulation of aspect ratio as well as the size of the innermost holes is also studied to show the influence of holes' size in combination with A on pursuing a nearly constant group index and to further investigate the tolerance of the design. Fig. 4 illustrates the systematic calculation of the product of group index (n_g) and normalized bandwidth ($\Delta\omega/\omega$) [16] covering a range of A from 0.6 to 2.0 and R from 0.92 to 1.08. The bandwidth $\Delta\omega$ is defined as the frequency range that is corresponding to the change of group index within ±10%, where the group index is considered constant [17]. The relative area ratio R is slightly tailored to represent a possible deviation of the area ratio caused by fabrication process. Fig. 4 indicates that a flat-band slow-light region can be traced at the maroon area where the product $n_g(\Delta\omega/\omega)$ [15] reaches its highest value above 0.3 and the group index keeps almost constant when A is around 1.6. The calculation shows under the condition that A is fixed at 1.6, when the increment of R is less than 4%, the product $n_g(\Delta\omega/\omega)$ remains almost constant, and when the R is slightly decreased to the range of 0.92–0.94, the product $n_g(\Delta\omega/\omega)$ slightly increases to 0.304. In other words, with slight R change within 10%, the product of $n_g(\Delta\omega/\omega)$ remains nearly constant at 0.3. This result reveals one of the advantages of such design, the robustness against the change of hole sizes, if a proper aspect ratio is chosen. This advantage can release the stringent requirement of controlling precise hole sizes during the fabrication process. Fig. 5 further explains the effect of aspect ratio combined with area change to achieve a nearly constant group index. When the hole area is fixed, in the flat-band

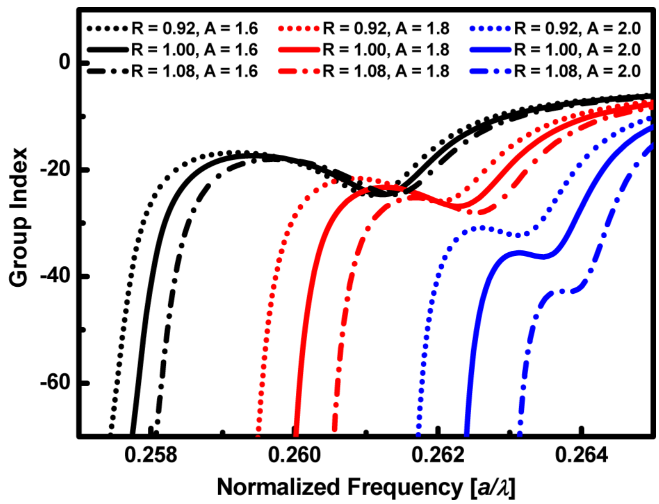

Fig. 5. Approaching constant group index with change of the relative area ratio R. When R is around 1.0, a nearly constant group index of 36 can be achieved with aspect ratio of 2.0.

region, the average group index increases and the fluctuation is reduced as aspect ratio increases; while under the same aspect ratio, a higher area ratio R can reduce the fluctuation. In a previously reported method by changing positions of first two rows of holes, the group index fluctuation in the flat-band region increases as the group index increases [17], which indicates the GVD increases at a higher group index. In comparison, in the proposed design the fluctuation of group index in the flat-band region remains almost to the same extent when the group index increases as shown in Fig. 5. With proper choice of aspect ratio, a vanishing GVD within ± 0.05 ns/(nm·cm) is achieved which is twice smaller than the data reported as in [13] under similar group index. Under such circumstances, an almost optimized flat band, which is marked correspondingly as the gray region in Fig. 2(b) and as the black solid curve in Fig. 5, with normalized bandwidth $(\Delta\omega/\omega)$ of 1.38%, can be achieved, and the maximum group index–bandwidth product $n_g(\Delta\omega/\omega)$ is 0.304.

IV. Conclusion

Slow-group-velocity photonic crystal waveguide with vanishing GVD by using capsule-shaped air holes on hexagonal lattice is proposed. Theoretical study on the effect of fine-tuning the aspect ratio of the innermost holes on flattening the GVD is briefly introduced. A nearly flat-band photonic crystal waveguides with group index of 21–36 over the normalized bandwidth $(\Delta\omega/\omega)$ of 1.38%–0.4% can be achieved with this design. In combination with the size tuning effect, group index in the range of 21–43 for normalized bandwidth about 1.5%–0.3% is obtained. The optimized design exhibits a nearly constant group index of 21 over 22.7 nm and 32 over 8 nm at $\lambda = 1.55$ μm, which corresponds to a 700 ps and 1.1 nsc delay time with bandwidth of 2.8 and 1 THz for a centimeter-long device, respectively. The proposed idea can lead to an alternative route to achieve flat band, and the studied effect can contribute an extra degree of freedom to the design and fabrication of slow-light photonic crystal slab waveguides with vanishing GVD.

References

[1] M. S. Moreolo, V. Morra, and G. Cincotti, "Design of photonic crystal delay lines based on enhanced coupled-cavity waveguides," *J. Opt. A–Pure Appl. Opt.*, vol. 10, pp. 064002-1–064002-6, Jun. 2008.
[2] C. J. Chang-Hasnain, P. C. Ku, J. Kim, and S. L. Chuang, "Variable optical buffer using slow light in semiconductor nanostructures," *Proc. IEEE*, vol. 91, no. 11, pp. 1884–1897, Nov. 2003.
[3] J. B. Khurgin, "Optical buffers based on slow light in electromagnetically induced transparent media and coupled resonator structures: Comparative analysis," *J. Opt. Soc. Amer. B–Opt. Phys.*, vol. 22, pp. 1062–1074, May 2005.
[4] S. F. Mingaleev, A. E. Miroshnichenko, Y. S. Kivshar, and K. Busch, "All-optical switching, bistability, and slow-light transmission in photonic crystal waveguide-resonator structures," *Phys. Rev. E*, vol. 74, pp. 046603-1–046603-15, Oct. 2006.
[5] M. Soljacic, S. G. Johnson, S. H. Fan, M. Ibanescu, E. Ippen, and J. D. Joannopoulos, "Photonic-crystal slow-light enhancement of nonlinear phase sensitivity," *J. Opt. Soc. Amer. B–Opt. Phys.*, vol. 19, pp. 2052–2059, Sep. 2002.
[6] R. Iliew, C. Etrich, T. Pertsch, and F. Lederer, "Slow-light enhanced collinear second-harmonic generation in two-dimensional photonic crystals," *Phys. Rev. B*, vol. 77, pp. 115124-1–115124-9, Mar. 2008.
[7] T. Baba, "Slow light in photonic crystals," *Nature Photon.*, vol. 2, pp. 465–473, Aug. 2008.
[8] E. Chow, S. Y. Lin, S. G. Johnson, P. R. Villeneuve, J. D. Joannopoulos, J. R. Wendt, G. A. Vawter, W. Zubrzycki, H. Hou, and A. Alleman, "Three-dimensional control of light in a two-dimensional photonic crystal slab," *Nature*, vol. 407, pp. 983–986, Oct. 2000.
[9] S. G. Johnson, S. H. Fan, P. R. Villeneuve, J. D. Joannopoulos, and L. A. Kolodziejski, "Guided modes in photonic crystal slabs," *Phys. Rev. B*, vol. 60, pp. 5751–5758, Aug. 1999.
[10] J. L. He, Y. Jin, Z. Hong, and S. L. He, "Slow light in a dielectric waveguide with negative-refractive-index photonic crystal cladding," *Opt. Exp.*, vol. 16, pp. 11077–11082, Jul. 2008.
[11] M. Notomi, K. Yamada, A. Shinya, J. Takahashi, C. Takahashi, and I. Yokohama, "Extremely large group-velocity dispersion of line-defect waveguides in photonic crystal slabs," *Phys. Rev. Lett.*, vol. 87, pp. 253902-1–253902-4, Dec. 2001.
[12] J. M. Brosi, J. Leuthold, and W. G. Freude, "Microwave-frequency experiments validate optical simulation tools and demonstrate novel dispersion-tailored photonic crystal waveguides," *J. Lightw. Technol.*, vol. 25, no. 9, pp. 2502–2510, Sep. 2007.
[13] A. Y. Petrov and M. Eich, "Zero dispersion at small group velocities in photonic crystal waveguides," *Appl. Phys. Lett.*, vol. 85, pp. 4866–4868, Nov. 2004.
[14] M. D. Settle, R. J. P. Engelen, M. Salib, A. Michaeli, L. Kuipers, and T. F. Krauss, "Flatband slow light in photonic crystals featuring spatial pulse compression and terahertz bandwidth," *Opt. Exp.*, vol. 15, pp. 219–226, Jan. 2007.
[15] L. H. Frandsen, A. V. Lavrinenko, J. Fage-Pedersen, and P. I. Borel, "Photonic crystal waveguides with semi-slow light and tailored dispersion properties," *Opt. Exp.*, vol. 14, pp. 9444–9450, Oct. 2006.
[16] S. Kubo, D. Mori, and T. Baba, "Low-group-velocity and low-dispersion slow light in photonic crystal waveguides," *Opt. Lett.*, vol. 32, pp. 2981–2983, Oct. 2007.
[17] J. Li, T. P. White, L. O'Faolain, A. Gomez-Iglesias, and T. F. Krauss, "Systematic design of flat band slow light in photonic crystal waveguides," *Opt. Exp.*, vol. 16, pp. 6227–6232, Apr. 2008.
[18] D. Mori and T. Baba, "Wideband and low dispersion slow light by chirped photonic crystal coupled waveguide," *Opt. Exp.*, vol. 13, pp. 9398–9408, Nov. 2005.
[19] S. G. Johnson, P. R. Villeneuve, S. H. Fan, and J. D. Joannopoulos, "Linear waveguides in photonic-crystal slabs," *Phys. Rev. B*, vol. 62, pp. 8212–8222, Sep. 2000.

Yun-Sheng Chen (S'08) received the M.S. degree in optics from the College of Optics and Photonics-Center for Research and Education in Optics and Lasers (CREOL), the University of Central Florida, Orlando. He is currently working toward the Ph.D. degree at the Department of Electrical and Computer Engineering, University of Texas at Austin, Austin.

His current research interests include photonic crystal waveguide, optical true time delay, and nanofabrication.

Yang Zhao (S'08) received the M.S. degree in optics from the College of Optics and Photonics-Center for Research and Education in Optics and Lasers (CREOL), the University of Central Florida, Orlando, in 2008. She is currently working toward the Ph.D. degree at the Department of Electrical and Computer Engineering, the University of Texas at Austin, Austin.

Her current research interests include Si photonics, optical phased array, and nanofabrication.

Amir Hosseini (S'05) received the B.Sc. degree (with honors) in electrical engineering from Sharif University of Technology, Tehran, Iran, in 2005, and the M.S. degree in electrical and computer engineering from Rice University, Houston, TX, in 2007. He is currently working toward the Ph.D. degree in optical interconnect group at the Department of Electrical and Computer Engineering, University of Texas at Austin, Austin.

He is currently engaged in research on optical-phased array technology and high-performance optical modulators design and optimizations. His current research interests include the design optimization for nanoscale manufacturability.

David Kwong received the B.S. degree in electrical engineering in 2006 from the University of Texas at Austin, Austin, where he is currently working toward the Master's degree in optical-phased array technology and optical modulation at the Optical Interconnect Group.

For two years, he was with Samsung Austin Semiconductor, where he was engaged in process integration for Dynamic RAM (DRAM)back-end-of-line (BEOL) processes.

Wei Jiang received the B.S. degree in physics from Nanjing University, Nanjing, China, in 1996, and the M.A. degree in physics and the Ph.D. degree in electrical and computer engineering from the University of Texas at Austin, Austin, in 2000 and 2005, respectively.

From 2004 to 2007, he held research positions with Omega Optics, Inc., Austin. Since September 2007, he has been an Assistant Professor with the Department of Electrical and Computer Engineering, Rutgers University, Piscataway, NJ. His current research interests include photonic crystals, silicon photonics, optical interconnects, and beam steering.

Seth R. Bank (S'95–M'06) received the B.S. degree from the University of Illinois at Urbana-Champaign (UIUC), Urbana, IL, in 1999, and the M.S. and Ph.D. degrees from Stanford University, Stanford, CA, in 2003 and 2006, respectively, all in electrical engineering.

He studied the fabrication of InGaP–GaAs and InGaAs–InP HBTs at UIUC. His Ph.D. research was focused upon the molecular beam epitaxy (MBE) growth, fabrication, and device physics of long-wavelength vertical cavity surface-emitting laser and low-threshold edge-emitting lasers in the GaInNAs(Sb)–GaAs material system. He was a Post doctoral Scholar with the University of California, Santa Barbara, during 2006, where his research centered on the growth of metal–semiconductor hetero- and nano-structures (e.g., ErAs nanoparticles in GaAs). He is currently an Assistant Professor of Electrical and Computer Engineering with the University of Texas at Austin, Austin. His current research interests include the MBE growth of novel heterostructures and nanocomposites and their application to silicon-based lasers, mid-infrared (IR) lasers, Terhertz (THz) generation and sensing, and high-speed/low-power transistors. He is the coauthor of more than 140 papers and presentations in these areas.

Dr. Bank is a recipient of the 2009 Presidential Early Career Award for Scientists and Engineers, the 2009 Young Scientist Award from the International Symposium on Compound Semiconductors, the 2008 Defense Advanced Research Projects Agency (DARPA) Young Faculty Award, the 2008 Young Investigator Award from the North American molecular beam epitaxy (MBE) Meeting, and several Best Paper Awards.

Emanuel Tutuc received the B.S. and M.S. degrees from the Ecole Normale Superieure, The University of Paris, Paris, France in 1997 and 1998, respectively, and the Ph.D. degree in 2004 from Princeton University, Princeton, NJ, in 2004, all in physics.

His Ph.D. research focused on the molecular beam epitaxy (MBE) growth of ultrahigh mobility electron systems, and the physics of interacting electron systems in two dimensions. Between 2004 and 2006, he was a Postdoctoral Researcher at IBM T.J. Watson Research Center, Yorktown Heights, NY, where his research centered on the growth and electronic properties of Si and Ge nanowires and heterostructures. He is currently an Assistant Professor of electrical and computer engineering at the University of Texas at Austin, Austin. His current research interests include the growth and electronic properties of semiconductor nanowires and graphene, and their application to high-speed/low-power transistors.

Dr. Tutuc is a recipient of the 2009 National Science Foundation (NSF) CAREER Award, the 2008 Defense Advanced Research Projects Agency (DARPA) Young Faculty Award, and the Charlotte Elizabeth Procter Fellowship (Princeton).

Ray T. Chen (S'92–M'91–SM'98–F'04) received the B.S. degree in physics from the National Tsing-Hua University, Hsinchu, Taiwan, in 1980, and the M.S. degree in physics and the Ph.D. degree in electrical engineering from the University of California, Oakland, in 1983 and 1988, respectively.

From 1988 to 1992, he was a Research Scientist, the Manager, and the Director of the Department of Electro-Optic Engineering, Physical Optics Corporation, Torrance, CA. In 1992, he joined the Electrical and Computer Engineering (ECE) Department, University of Texas (UT) at Austin, Austin, as a faculty to start optical interconnect research program, where he currently holds the Cullen Trust for Higher Education Endowed Professorship and is also the Director of the Nanophotonics and Optical Interconnects Research Laboratory, Microelectronics Research Center. He is also the Director of a newly formed Air Force Office of Scientific Research (AFOSR) Multi-Disciplinary Research Initiative (MURI) Center for Silicon Nanomembrane, which involves faculty from Stanford, UIUC, Rutgers, and UT Austin. He is the Chief Technical Officer (CTO)/founder of Radiant Research, where he was the Chair of the Board 2000 to 2001. He is also the founder of Omega Optics, Inc., where he has been the Chair of the Board since 2001. He has authored or coauthored more than 510 published articles, including more than 80 invited papers. He holds 18 issued patents. He was an Editor, a Co-Editor, or a coauthor for 22 books. He has also been a consultant for various federal agencies and private companies.

Prof. Chen has chaired or been a program-committee member for more than 90 domestic and international conferences organized by the IEEE and The International Society of Optical Engineering (SPIE), the Optical Society of America (OSA), and the Photonics Society of Chinese Americans (PSC). He has delivered numerous invited talks to professional societies. He is a Fellow of the OSA and the SPIE. He was the recipient of the 1987 University of Carolina (UC) Regent's Dissertation Fellowship and the 1999 UT Engineering Foundation Faculty Award for his contributions in research, teaching, and services. He received the IEEE Teaching Award in 2008. In 1979, he led a university debate team of the National Tsing-Hua University, which received the National Championship of National Debate Contest in Taiwan.